Influences of Crystal Structures and Molecular Sizes on the Charge Mobility of Organic Semiconductors: Oligothiophenes

Xiaodi Yang,[†] Linjun Wang,[†] Caili Wang,[†] Wei Long,[†] and Zhigang Shuai*,[†,‡]

Key Laboratory of Organic Solids, Beijing National Laboratory for Molecular Science, Institute of Chemistry, Chinese Academy of Sciences, 100190 Beijing, China, and Department of Chemistry, Tsinghua University, 100084 Beijing, China

Received January 23, 2008. Revised Manuscript Received February 29, 2008

Both crystal packing and molecular size have strong influences on the charge mobility for organic semiconductors. The crystal structures for oligothiophene (*n*T) can be roughly classified into two types: the $Z = 2$ (two molecules in one unit cell) or high temperature (HT) phase and the $Z = 4$ or low temperature (LT) phase. Through first-principles calculations within the Marcus electron transfer theory coupled with random walk simulation for room temperature charge diffusion constants, we found that the hole mobility of the HT phase is about 3–4 times larger than that of the LT phase because the molecular packing in the HT phase favors the hole transfer (i.e., the frontier orbital wave function phases of the dimer are constructive, which tends to maximize the overlap), while for the LT phase, the molecules are packed in a position that reduces the intermolecular orbital overlap due to phase cancellation. As the molecular size increases from 2T to 8T, the hole mobility tends to increase because the reorganization energy decreases with the chain length.

Introduction

Organic semiconductors based on π-conjugated oligomers and polymers constitute the active elements in (opto)electronic devices, such as light-emitting diodes (OLED),[1] field-effect transistors (FETs),[2] or solar cells.[3] The advantages of organic electronic materials are a low cost, versatility of chemical synthesis, ease of processing, and flexibility. Charge transport behavior in organic materials is of great interest.[4] The main parameters to characterize the performance of a semiconducting FET are its carrier mobility and on/off current ratio. For inorganic semiconductor Si single crystals, the room temperature mobility can reach as high as a few 10^2 to approximately a few 10^3 cm^2/V s.[5] Traditionally, the organic materials usually possess a very low mobility (10^{-6} to $\sim 10^{-4}$). Recent progresses demonstrated that the mobility of approximately a few tenths of a cm^2/V s can be realized in organic FET devices,[6] and even larger values of approximately a few tens of cm^2/V s have been reported.[7]

Oligothiophene is one of the earliest organic materials for organic thin film FETs.[8,9] Thiophene-based materials exhibit a variety of intra- and intermolecular interactions—van der Vaals interactions, weak hydrogen bondings, $\pi-\pi$ stacking, and sulfur−sulfur interactions—originating form the high polarizability of sulfur electrons in the thiophene rings.[10] Therefore, thiophene oligomers can be regarded as a versatile building block for organized structures. The charge transport properties critically depend on the relative orientations and solid-state packing of the species involved.[11,12] It has been

* Corresponding author. Tel.: +86-10-62521934; fax: +86-10-62525573; e-mail: zgshuai@iccas.ac.cn.
† Beijing National Laboratory for Molecular Science.
‡ Tsinghua University.

(1) (a) Zojer, E.; Pogantsch, A.; Hennebicq, E.; Beljonne, D.; Brédas, J. L.; de Freitas, P. S.; Scherf, U.; List, E. J. W. *J. Chem. Phys.* **2002**, *117*, 6794. (b) Chen, A. C. A.; Culligan, S. W.; Geng, Y.; Chen, S. H.; Klubek, K. P.; Vaeth, K. M.; Tang, C. W. *Adv. Mater.* **2004**, *16*, 783. (c) Friend, R. H.; Gymer, R. W.; Holmes, A. B.; Burroughes, J. H.; Marks, R. N.; Taliani, C.; Bradley, D. D. C.; Dos Santos, D. A.; Brédas, J. L.; Lögdlund, M.; Salaneck, W. R. *Nature (London, U.K.)* **1999**, *397*, 121.

(2) (a) Horowitz, G.; Hajlaoui, M. E. *Adv. Mater.* **2000**, *12*, 1046. (b) Nagamatsu, S.; Kaneto, K.; Azumi, R.; Matsumoto, M.; Yoshida, Y.; Yase, K. *J. Phys. Chem. B* **2005**, *109*, 9374.

(3) (a) Spanggaard, H.; Krebs, F. C. *Sol. Energy Mater Sol. Cells* **2004**, *83*, 125. (b) Smith, A. P.; Smith, R. R.; Taylor, B. E.; Durstock, M. F. *Chem. Mater.* **2004**, *16*, 4687. (c) Padinger, F.; Rittberger, R. S.; Sariciftci, N. S. *Adv. Funct. Mater.* **2003**, *13*, 85.

(4) (a) Pope, K.; Swenberg, C. E. *Electronic Processes in Organic Crystals and Polymers*, 2nd ed.; Oxford University Press: New York, 1999. (b) Silinsh, E. A.; Čápek, V. *Organic Molecular Crystals: Interaction, Localization, and Transport Phenomena*; AIP: New York, 1994. (c) Gershenson, M. E.; Podzorov, V.; Morpurgo, A. F. *Rev. Mod. Phys.* **2006**, *78*, 973.

(5) Beadle, W. F.; Tsai, J. C. C.; Plummer, R. D. *Quick Reference Manual of Semiconductor Engineers*; Wiley: New York, 1985.

(6) Newman, C. R.; Frisbie, C. D.; da Silva Filho, D. A.; Brédas, J. L.; Ewbank, P. C.; Mann, K. R. *Chem. Mater.* **2004**, *16*, 4436.

(7) (a) Sundar, V. C.; Zaumseil, J.; Podzorov, V.; Menard, E.; Willett, R. L.; Someya, T.; Gershenson, M. E.; Rogers, J. A. *Science (Washington, DC, U.S.)* **2004**, *303*, 1644. (b) Podzorov, V.; Menard, E.; Borissov, A.; Kiryukhin, V.; Rogers, J. A.; Gershenson, M. E. *Phys. Rev. Lett.* **2004**, *93*, 86602.

(8) (a) Fichou, D. *Handbook of Oligo- and Polythiophenes*; Wiley-VCH: New York, 1999. (b) Fichou, D. *J. Mater. Chem.* **2000**, *10*, 571.

(9) (a) Schoonveld, W. A.; Wildeman, J.; Fichou, D.; Bobbert, P. A.; van Wees, B. J.; Klapwijk, T. M. *Nature (London, U.K.)* **2000**, *404*, 977. (b) Melucci, M.; Gazzano, M.; Barbarella, G.; Cavallini, M.; Biscarini, F.; Maccagnani, P.; Ostoja, P. *J. Am. Chem. Soc.* **2003**, *125*, 10266. (c) Dinelli, F.; Murgia, M.; Levy, P.; Cavallini, M.; Biscarini, F.; de Leeuw, D. M. *Phys. Rev. Lett.* **2004**, *92*, 116802.

(10) (a) Marseglia, E. A.; Grepioni, F.; Tedesco, E.; Braga, D. *Mol. Cryst. Liq. Cryst.* **2000**, *348*, 137. (b) Barbarella, G.; Zambianchi, M.; Bongini, A.; Antolini, L. *Adv. Mater.* **1993**, *5*, 834.

(11) (a) Cheng, Y. C.; Silbey, R. J.; da Silva, D. A.; Calbert, J. P.; Cornil, J.; Brédas, J. L. *J. Chem. Phys.* **2003**, *118*, 3764. (b) Brédas, J. L.; Beljonne, D.; Cornil, J.; Calbert, J. P.; Shuai, Z.; Silbey, R. *Synth. Met.* **2001**, *125*, 107.

(12) (a) Hutchison, G. R.; Ratner, M. A.; Marks, T. J. *J. Am. Chem. Soc.* **2005**, *127*, 16866. (b) Cornil, J.; Beljonne, D.; Calbert, J. P.; Brédas, J. L. *Adv. Mater.* **2001**, *13*, 1053.

10.1021/cm8002172 CCC: $40.75
Published on Web 04/11/2008

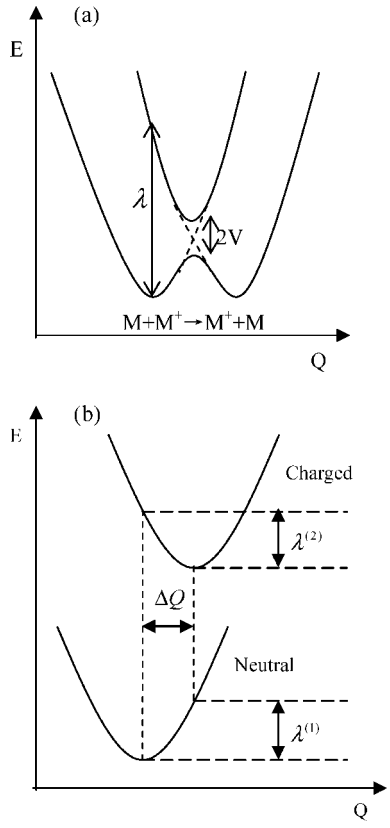

Figure 1. Schematic representation of (a) hole transfer through a transition state by weak (nonadiabatic) coupling and (b) adiabatic energy surfaces corresponding to the ionization process. ΔQ is the NM displacement, and the two energetic terms λ_1 and λ_2 define the internal reorganization energy.

shown that the intermolecular interactions and molecular reorganization energy upon accepting/donating a charge can strongly influence the charge mobility.[12,13]

Oligothiophenes exhibit a herringbone structure in the crystal form. However, depending on the sublimation temperatures for 4T and 6T, there exist two different types of structures. For the high source temperature grown crystal, there are two molecules in one unit cell ($Z = 2$) for 2T, 4T, and 6T. For the low temperature phase, there are four molecules ($Z = 4$) in one unit cell for 4T, 6T, 7T, and 8T. In addition, for 3T, there are eight molecules in one unit cell. Thus, various crystal structures provide an ideal system to study the molecular packing effects on electron transport. In addition, the molecular size is well-defined in terms of the number of thiophene rings. It is intriguing to see as to how the size of the conjugated molecule affects the charge motion. Previous experimental FET device measurements have given the hole mobility in the range of 2×10^{-7} to $0.3\ \mathrm{cm^2\ V^{-1}\ s^{-1}}$ for the thin film and crystalline phases.[14] Through our theoretical study, the intrinsic transport behavior in oligothiophenes was revealed, which can shed light on the diversified range of experimental values.

Table 1. DFT-B3LYP/6-31G* Calculated Reorganization Energies λ (meV) by Adiabatic Potential Surfaces of the Neutral and Cation Species and by NM Analysis

	reorganization energy	
molecules	adiabatic potential	normal mode
2T	361	364
3T	316	323
4T	286	288
5T	265	274
6T	244	255
7T	224	238
8T	203	212

Computational Approaches

Generally speaking, there are two types of carrier motion in the solid state: (i) the coherent band model and (ii) the incoherent hopping model. Electronic band structure calculations previously have been used to predict charge transport in perfectly ordered materials at very low temperatures. The band model is usually suitable for inorganic semiconductors where the interaction between different sites is through strong valence bonds. At high temperatures, the dynamic structure disorder may strongly localize the charge, thus invalidating the band transport model, suggesting that hopping may be the dominant mechanism, especially for organic materials. Here, we adopt the hopping mechanism as advocated by Brédas et al.,[13] Hutchison et al.,[12a] and Deng and Goddard.[15]

The charge transport process (for holes) between two adjacent molecules follows the reaction $M + M^+ \rightarrow M^+ + M$, where M is the molecule undergoing the hole transfer. The hopping rate can be described by Marcus theory by the following equation:[16]

$$k = \frac{V^2}{\hbar}\left(\frac{\pi}{\lambda k_B T}\right)^{1/2} \exp\left(-\frac{\lambda}{4k_B T}\right) \quad (1)$$

There are two major parameters that determine the self-exchange electron transfer (ET) rate: the intermolecular transfer integral (V) and the reorganization energy (λ) (see Figure 1a). Eq 1 is applicable for $V \ll \lambda$. The charge transport process is considered to be a cross-barrier classical mechanics motion, with a barrier height of $\lambda/4$. The reaction coordinate Q in Figure 1a is an ensemble of geometric deformations of the dimer system. The reorganization energy includes the molecular geometry modifications when an electron is added or removed from a molecule (inner reorganization) as well as the modifications in the surrounding medium due to polarization effects (outer reorganization). Here, we focus on the inner reorganization energy, which reflects the geometric changes in the molecules when going from the neutral to the ionized state and vice versa. It is the sum of two relaxation energy terms:[17] (i) the difference between the energies of the neutral molecule in its equilibrium geometry and in the relaxed geometry characteristic of the ion and (ii) the difference between the energies of the radical ion in its equilibrium geometry and in the neutral geometry, as

(13) (a) Coropceanu, V.; Cornil, J.; da Silva Filho, D. A.; Olivier, Y.; Silbey, R.; Brédas, J. L. *Chem. Rev.* **2007**, *107*, 926. (b) Brédas, J. L.; Calbert, J. P.; da Silva Filho, D. A.; Cornil, J. *Proc. Natl. Acad. Sci. U.S.A.* **2002**, *99*, 5804.

(14) (a) Hajlaoui, R.; Fichou, D.; Horowitz, G.; Nessakh, B.; Constant, M.; Garnier, F. *Adv. Mater.* **1997**, *9*, 557. (b) Akimichi, H.; Waragai, K.; Hotta, S.; Kano, H.; Sakaki, H. *Appl. Phys. Lett.* **1991**, *58*, 1500. (c) Horowitz, G.; Peng, X. Z.; Fichou, D.; Garnier, F. *J. Mol. Electron.* **1991**, *7*, 85. (d) Katz, H. E.; Torsi, L.; Dodabalapur, A. *Chem. Mater.* **1995**, *7*, 2235. (e) Hajlaoui, R.; Horowitz, G.; Garnier, F.; Arce-Brouchet, A.; Laigre, L.; El Kassmi, A.; Demanze, F.; Kouki, F. *Adv. Mater.* **1997**, *9*, 389. (f) Hajlaoui, M. E.; Garnier, F.; Hassine, L.; al Kouki, F.; Bouchriha, H. *Synth. Met.* **2002**, *129*, 215.

(15) Deng, W. Q.; Goddard, W. A., III *J. Phys. Chem. B* **2004**, *108*, 8614.

(16) (a) Marcus, R. A. *Annu. Rev. Phys. Chem.* **1964**, *15*, 155. (b) Marcus, R. A. *Rev. Mod. Phys.* **1993**, *65*, 599.

(17) (a) Berlin, Y. A.; Hutchinson, G. R.; Rempala, P.; Ratner, M. A.; Michl, J. *J. Phys. Chem. A* **2003**, *107*, 3970. (b) Coropceanu, V.; Malagoli, M.; da Silva Filho, D. A.; Gruhn, N. E.; Bill, T. G.; Brédas, J. L. *Phys. Rev. Lett.* **2002**, *89*, 275503.

shown in Figure 1b. The λ terms are evaluated in two ways: (i) directly from the adiabatic potential-energy surfaces of neutral/cation and neutral/anion species[18] and (ii) from the normal-mode analysis, which provides the partition of the total relaxation energy into the contributions from each vibrational mode:[19]

$$\lambda = \sum \lambda_i = \sum \hbar\omega_i S_i \tag{2}$$

$$\lambda_i = \frac{k_i}{2}\Delta Q_i^2 \tag{3}$$

Here, the summations run over all the vibrational normal modes. ΔQ_i represents the displacement along normal mode (NM) i between the equilibrium geometries of the neutral and charged molecules, k_i and ω_i are the corresponding force constants and vibrational frequencies, and S_i denotes the Huang–Rhys factor measuring charge−phonon coupling strength .We calculated the reorganization energies at the density functional theory (DFT) level using the B3LYP functional and 6-31G* basis set. The NM analysis and Huang–Rhys factors as well as λ_i were obtained through the DUSHIN program.[20]

The electronic coupling terms were evaluated for the nearest neighbor molecules. Here, we took the single crystal structures of oligothiophenes to generate all possible intermolecular hopping pathways. The couplings between all these pairs were calculated through the diabatic model. The two diabatic states correspond to the carrier localized on the electron donating and accepting molecules, respectively. The electronic coupling can be obtained either by Koopmans' theorem at the Hartree–Fock mean-field level (indirect method)[12,21] or by direct dimer Hamiltonian evaluation method.[22,23] In the former case, it is cautioned that when the dimer is not cofacial, the site energy correction and the intermolecular overlap due to the crystal environment should be taken into account.[24]

The electronic coupling for hole transfer in the direct scheme can be written as

$$V = \left\langle \phi_{\mathrm{HOMO}}^{0,\mathrm{site1}} | F | \phi_{\mathrm{HOMO}}^{0,\mathrm{site2}} \right\rangle \tag{4}$$

where $\phi_{\mathrm{HOMO}}{}^{0,\mathrm{site1}}$ and $\phi_{\mathrm{HOMO}}{}^{0,\mathrm{site2}}$ represent the HOMOs of isolated molecules 1 and 2, respectively, and F is the Fock operator for the dimer with a density matrix from noninteracting dimer of $F = SC\varepsilon C^{-1}$, where S is the intermolecular overlap matrix, and C and ε are the molecular orbital coefficients and energies from one-step diagonalization without iteration. This calculation was performed using the PW91PW91/6-31G* basis set. It has been shown that this choice of functional gives the best results at the DFT level.[25] In the case of the pentacene dimer from cofacial to perpendicular edge-corner packing, namely, the relative tilt angle from 0 to 90°, we compared eq 4 with the site energy and overlap corrected splitting scheme of Valeev et al.[24] We have shown that both give almost identical results for the whole range of tilt angles.[26] The one-step diagonalization for eq 4 is simple, efficient, and reliable.

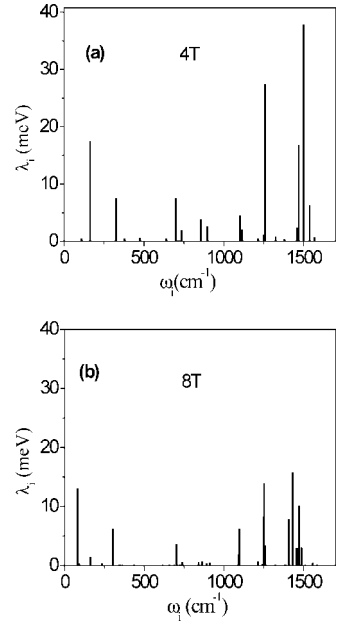

Figure 2. Contribution of the vibrational modes to the cationic relaxation energy for molecules 4T (a) and 8T (b).

Here, we model the charge transport as a Brownian motion process, as described by a particle diffusion process. The mobility can be expressed by the Einstein equation[27]

$$\mu = \frac{e}{k_B T} D \tag{5}$$

where $D$is the isotropic charge diffusion constant. It is simulated by the random walk technique. We took the molecular crystal as a reference structure and any given molecule as the initial charge center. The charge is only allowed to hop between nearest neighbor molecules. The hopping rate k for a specific pathway is calculated through eq 1. The hopping probability was evaulated as $p_\alpha = k^\alpha/\sum_\alpha k^\alpha$. The denominator is a sum over all the possible hopping pathways. The hopping time along this direction is $1/k^\alpha$, and the hopping distance is taken to be the intermolecular center distance. At each step in the simulation, a random number r is generated, uniformly distributed between 0 and 1. If $\sum_{\alpha=1}^{j-1} p_\alpha < r \le \sum_{\alpha=1}^{j} p_\alpha$ (accumulated probability), then the charge is allowed to go along the jth direction. Each simulation lasts from a few

(18) (a) Malagoli, M.; Brédas, J. L. *Chem. Phys. Lett.* **2000**, *327*, 13. (b) Lemaur, V.; da Silva Filho, D. A.; Coropceanu, V.; Lehmann, M.; Geerts, Y.; Piris, J.; Debije, M. G.; van de Craats, A. M.; Senthilkumar, K.; Siebbeles, L. D. A.; Warman, J. M.; Brédas, J. L.; Cornil, J. *J. Am. Chem. Soc.* **2004**, *126*, 3271.
(19) (a) Kwon, O.; Coropceanu, V.; Gruhn, N. E.; Durivage, J. C.; Laquindanum, J. G.; Katz, H. E.; Cornil, J.; Brédas, J. L. *J. Chem. Phys.* **2004**, *120*, 8186. (b) Sanchez-Carrera, R. S.; Coropceanu, V.; da Silva Filho, D. A.; Friedlein, R.; Osikowicz, W.; Murdey, R.; Suess, C.; Salaneck, W. R.; Brédas, J. L. *J. Phys. Chem. B* **2006**, *110*, 18904. (c) Brédas, J. L.; Beljonne, D.; Coropceanu, V.; Cornil, J. *Chem. Rev.* **2004**, *104*, 4971.
(20) (a) Weber, P.; Reimers, J. R. *J. Phys. Chem. A* **1999**, *103*, 9830. (b) Cai, Z. L.; Reimers, J. R. *J. Phys. Chem. A* **2000**, *104*, 8389.
(21) Lin, B. C.; Cheng, C. P.; You, Z. Q.; Hsu, C. P. *J. Am. Chem. Soc.* **2005**, *127*, 66.
(22) Troisi, A.; Orlandi, G. *Chem. Phys. Lett.* **2001**, *344*, 509.
(23) Yin, S. W.; Yi, Y. P.; Li, Q. X.; Yu, G.; Liu, Y. Q.; Shuai, Z. G. *J. Phys. Chem. A* **2006**, *110*, 7138.
(24) (a) Valeev, E. F.; Coropceanu, V.; da Silva Filho, D. A.; Salman, S.; Brédas, J. L. *J. Am. Chem. Soc.* **2006**, *128*, 9882. (b) Grzegorczyk, W. J.; Savenije, T. J.; Valeton, J. J. P.; Fratiloiu, S.; Grozema, F. C.; de Leeuw, D. M.; Siebbeles, L. D. A. *J. Phys. Chem. C* **2007**, *111*, 18411. (c) Prins, P.; Senthilkumar, K.; Grozema, F. C.; Jonkheijm, P.; Schenning, A. P. H. J.; Meijer, E. W.; Siebbeles, L. D. A. *J. Phys. Chem. B* **2005**, *109*, 18267.
(25) (a) Huang, J. S.; Kertesz, M. *Chem. Phys. Lett.* **2004**, *390*, 110. (b) Song, Y. B.; Di, C. A.; Yang, X. D.; Li, S. P.; Xu, W.; Liu, Y. Q.; Yang, L. M.; Shuai, Z. G.; Zhang, D. Q.; Zhu, D. B. *J. Am. Chem. Soc.* **2006**, *128*, 15940.
(26) Yang, X. D.; Li, Q. K.; Shuai, Z. G. *Nanotechnology* **2007**, *18*, 424029.
(27) Schein, L. B.; McGhie, A. R. *Phys. Rev. B: Condens. Matter Mater. Phys.* **1979**, *20*, 1631.

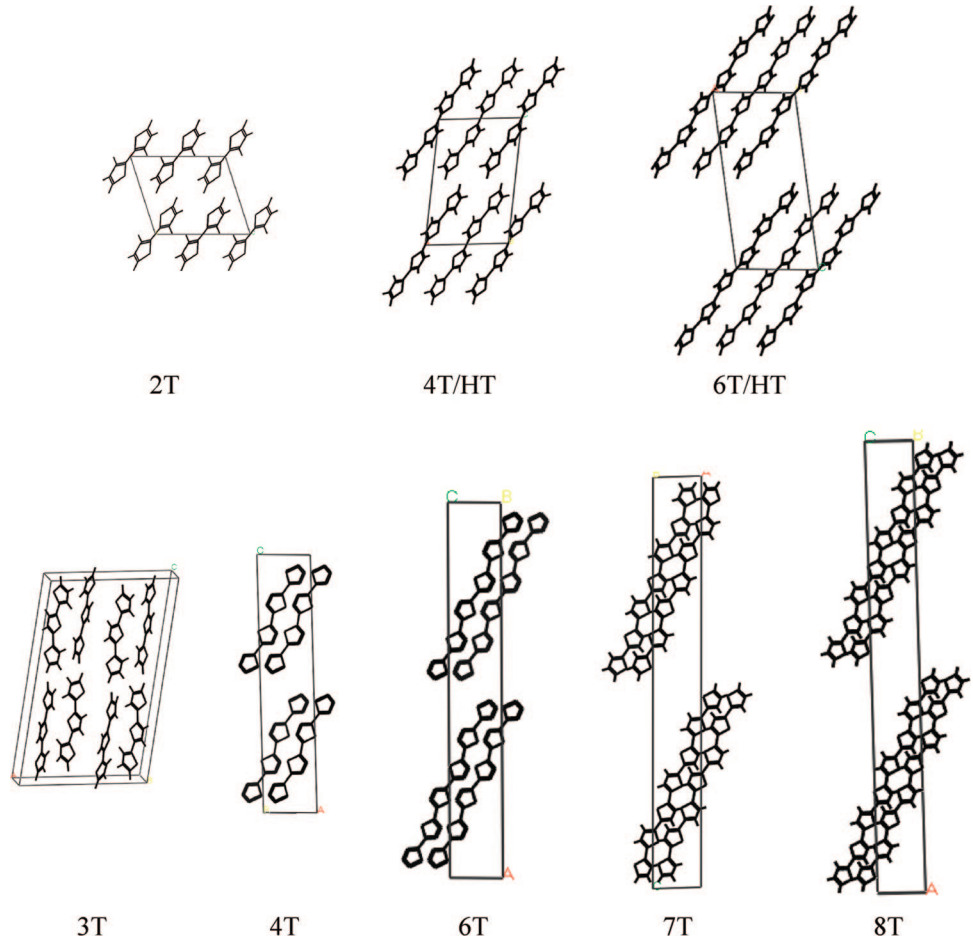

Figure 3. Crystal structures of α-*n*Ts.

tens to a few hundreds of a microsecond. Then, the diffusion constant is obtained as $D = \lim_{t\to\infty} \langle l(t)^2\rangle/6t$, where $l(t)^2$ is the mean squared displacement. Two thousand trajectories were simulated to obtain a converged diffusion constant, namely, a linear relationship between the square of the diffusion distance and the diffusion time. The details of simulation are given in the Supporting Information.

The basic assumption is that the charge transport is a slow process where the solvent (surrounding molecules) and the solute molecule (with charge) have enough time to equilibrate. This is pertinent for the soft organic system. All the quantum chemistry calculations were performed with the Gaussian 03 package.[28]

Results and Discussion

In the crystalline form of α-oligothiophenes, all of them are quasi-planar, the inter-ring torsion angle being below the measurement accuracy (<1°). One exception is α-3T, for which a slight deviation from planarity (6–9°) was reported in the crystal form.[29] Table 1 displays the reorganization energies calculated for positive polarons of oligothiophene from the adiabatic potentials and from the NM analysis. The λ values obtained from both approaches are very close. This indicates that the charge reorganizing process can be well-described by the harmonic oscillator model as assumed in Marcus theory. It is also seen that the reorganization energy decreases as the chain is elongated.

We took the 4T and 8T molecules as examples to visualize the vibronic interactions for charge relaxation. NM analysis was performed at the B3LYP/6-31G* level. The results are displayed in Figure 2. The partition of the relaxation energies of these molecules into the contributions of each normal mode is displayed. It is seen that the contributions from the high frequency parts (1200–1600 cm^{-1}) decrease remarkably when going from 4T to 8T. These are the C−C single and double bond stretching modes, responsible for Raman processes, that are influenced by the conjugation length, as demonstrated previously.[30] Both the total molecular reorganization energies from 2T to 8T and the vibrational mode

(28) Frisch, M. J.; Trucks, G. W.; Schlegel, H. B.; Scuseria, G. E.; Robb, M. A.; Cheeseman, J. R.; Montgomery, J. A., Jr.; Vreven, T.; Kudin, K. N.; Burant, J. C.; Millam, J. M.; Iyengar, S. S.; Tomasi, J.; Barone, V.; Mennucci, B.; Cossi, M.; Scalmani, G.; Rega, N.; Petersson, G. A.; Nakatsuji, H.; Hada, M.; Ehara, M.; Toyota, K.; Fukuda, R.; Hasegawa, J.; Ishida, M.; Nakajima, T.; Honda, Y.; Kitao, O.; Nakai, H.; Klene, M.; Li, X.; Knox, J. E.; Hratchian, H. P.; Cross, J. B.; Bakken, V.; Adamo, C.; Jaramillo, J.; Gomperts, R.; Stratmann, R. E.; Yazyev, O.; Austin, A. J.; Cammi, R.; Pomelli, C.; Ochterski, J. W.; Ayala, P. Y.; Morokuma, K.; Voth, G. A.; Salvador, P.; Dannenberg, J. J.; Zakrzewski, V. G.; Dapprich, S.; Daniels, A. D.; Strain, M. C.; Farkas, O.; Malick, D. K.; Rabuck, A. D.; Raghavachari, K.; Foresman, J. B.; Ortiz, J. V.; Cui, Q.; Baboul, A. G.; Clifford, S.; Cioslowski, J.; Stefanov, B. B.; Liu, G.; Liashenko, A.; Piskorz, P.; Komaromi, I.; Martin, R. L.; Fox, D. J.; Keith, T.; Al-Laham, M. A.; Peng, C. Y.; Nanayakkara, A.; Challacombe, M.; Gill, P. M. W.; Johnson, B.; Chen, W.; Wong, M. W.; Gonzalez, C.; Pople, J. A. *Gaussian 03, revision C.02*; Gaussian, Inc.: Wallingford, CT, 2004.

contributions are in good agreement with the recent calculations performed by da Silva Filho et al.[31]

The crystal structure of α-*n*Ts is the herringbone arrangement, which is quite common in chain molecule crystals. All nonsubstituted α-*n*Ts crystallize in the monoclinic system with a $P2_1$ space group. The number of molecules per unit cell is $Z = 2$ for α-2T[32] and $Z = 8$ for α-3T,[29] while it is $Z = 4$ for α-7T[33] and α-8T.[34] The first α-6T single crystals were obtained by Siegrist et al. from the melt at high temperature (α-6T/HT)[35]and by Horowitz et al. using a sublimation technique (6T/LT).[36] Surprisingly, these two kinds of crystals have two different structures. Up to now, two different structures were identified for both α-4T and α-6T. In these two cases, the HT phase is $Z = 2$, while the others adopt a $Z = 4$ structure. The two crystal forms differ not only by the number of molecules in the unit cell but also by the way they pack. We depicted all the α-*n*T crystal forms in Figure 3. A view along the *b*-axis shows that 2T, 4T/HT,[37]and 6T/HT have the same packing structure. The crystal form of 4T/LT,[38] 6T/LT, 7T, and 8T shows the same packing form. The difference between these two kinds of packing structures lies in the tilt angle of the long axis of the molecule with respect to the normal of the plane of highest density, which is higher for $Z = 2$ than for $Z = 4$.[37]

The various types of charge hopping pathways are shown in Figure 4, as examples for 4T/HT ($Z = 2$) (Figure 4a) and 4T/LT ($Z = 4$) (Figure 4b). Figure 4 (a)-1,(b)-1 displays the nearest neighbor dimer pairs in the same molecular layer, which is the herringbone arrangement. Shown in Figure 4(a)-2,(b)-2 are head-to-tail stackings. Note that 2T, 4T/HT, and 6T/HT have the same packing structure. We then calculated all the 12 types of transfer integrals through the direct evaluation method of eq 4 for these three cases, which are displayed in Table 2. For the other packing structures (with $Z = 4$) of 4T/LT, 6T/LT, 7T, and 8T, the corresponding results are reported in Table 3. 3T is an exception, where $Z = 8$. Its packing structure is different from all other oligothiophene crystals. The nearest neighbor dimer and the hopping routes are shown in Figure 4c, and the transfer integrals are given in Table 3.

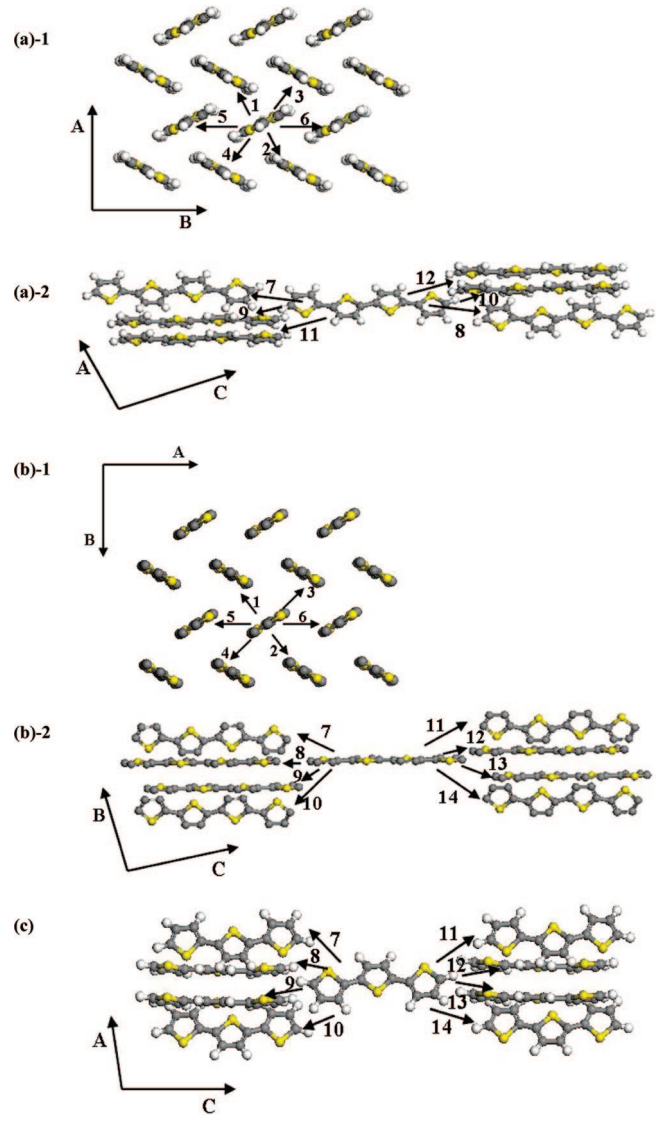

Figure 4. Charge hopping pathways schemes for 4T/HT (a), 4T (b), and 3T (c). Panels (a)-1 and (b)-1 display the hopping routes in the same molecular layer, and panels (a)-2 and (b)-2 are between different molecular layers. The crystal structure of 3T is different from all other crystals for the hoppings between different layers.

Table 2. DFT/PW91PW91/6-31G* Electronic Coupling Terms *V* (meV) for All Pathways for $Z = 2$ Structures of 2T, 4T/HT, and 6T/HT[a]

	2T		4T/HT		6T/HT	
pathway	*V*	*d*	*V*	*d*	*V*	*d*
1	34	5.34	40	5.31	36	5.38
5	6	5.90	4	5.75	3	5.68
7	1	10.00	0.7	17.82	0.4	25.68
9	12	8.31	2	15.81	0.7	23.38

[a] Corresponding intermolecular center-to-center distance *d* is in angstroms. By symmetry, pathways 2−4 are the same as 1, 6 as 5, 8 as 7, and 10−12 as 9.

If we compare Tables 2 and 3, it is immediately concluded that the largest electronic coupling term for the HT phase is about 34−40 meV, which is about twice as much as that for the LT phase, and among the LT or HT structures themselves, the coupling term values are close each other. For

(29) van Bolhuis, F.; Wynberg, H.; Havinga, E. E.; Meijer, E. W.; Starling, E. G. J. *Synth. Met.* **1989**, *30*, 381.
(30) Zerbi, G.; Siesler, H. W.; Noda, I.; Tasumi, M.; Krimm, S. *Modern Polymer Spectroscopy*; Wiley: New York, 1999.
(31) da Silva Filho, D. A.; Coropceanu, V.; Fichou, D.; Gruhn, N. E.; Bill, T. G.; Gierschner, J.; Cornil, J.; Brédas, J. L. *Philos. Trans. R. Soc. London, Ser. A* **2007**, *365*, 1435–1452.
(32) Chaloner, P. A.; Gunatunga, S. R.; Hitchcock, P. B. *Acta Crystallogr., Sect. C: Cryst. Struct. Commun.* **1994**, *50*, 1941.
(33) Azumi, R.; Goto, M.; Honda, K.; Matsumoto, M. *Bull. Chem. Soc. Jpn.* **2003**, *76*, 1561.
(34) Fichou, D.; Bachet, B.; Demanze, F.; Billy, I.; Horowitz, G.; Garnier, F. *Adv. Mater.* **1996**, *8*, 500.
(35) Siegrist, T.; Fleming, R. M.; Haddon, R. C.; Laudise, R. A.; Lovinger, A. J.; Katz, H. E.; Bridenbaugh, P.; Davis, D. D. *J. Mater. Res.* **1995**, *10*, 2170.
(36) Horowitz, G.; Bachet, B.; Yassar, A.; Lang, P.; Demanze, F.; Fave, J. L.; Garnier, F. *Chem. Mater.* **1995**, *7*, 1337.
(37) Antolini, L.; Horowitz, G.; Kouki, F.; Garnier, F. *Adv. Mater.* **1998**, *10*, 382.
(38) Siegrist, T.; Kloc, C.; Laudise, R. A.; Katz, H. E.; Haddon, R. C. *Adv. Mater.* **1998**, *10*, 379.
(39) Facchetti, A.; Mushrush, M.; Yoon, M.; Hutchison, G. R.; Ratner, M. A.; Marks, T. J. *J. Am. Chem. Soc.* **2004**, *126*, 13859.
(40) Servet, B.; Horowitz, G.; Ries, S.; Lagorsse, O.; Alnot, P.; Yassar, A.; Deloffre, F.; Srivastava, P.; Hajlaoui, R.; Lang, P.; Garnier, F. *Chem. Mater.* **1994**, *6*, 1809.
(41) Dodabalapur, A.; Torsi, L.; Katz, H. E. *Science (Washington, DC, U.S.)* **1995**, *268*, 270.

Table 3. DFT/PW91PW91/6-31G* Calculated Electronic Coupling Terms V (meV) for All Hopping Pathways of Other Than $Z = 2$ Crystal Phases for 3T, 4T, 6T, 7T, and 8T[a]

	3T		4T		6T		7T		8T	
pathway	V	d	V	d	V	d	V	d	V	d
1	7	4.67	12	4.93	18	4.98	18	4.81	17	4.92
2	13	5.06	17	5.01	16	4.92	14	4.97	17	4.96
3	13	4.72	17	5.01	16	4.92	17	4.82	17	4.96
4	13	5.06	12	4.93	18	4.98	18	4.97	17	4.92
5	0.4	5.64	18	6.08	10	6.03	13	5.95	9	6.00
6	0.4	5.64	18	6.08	10	6.03	13	5.95	9	6.00
7	2	12.16	5	16.49	2	24.18	0.4	28.82	1	31.88
8	4	13.25	3	17.63	2	25.34	0.4	29.67	0	30.73
9	4	13.20	4	15.55	3	23.16	1	27.68	0.5	32.95
10	19	12.29	0.0	16.96	0.0	24.51	0.3	28.84	0	32.13
11	0	14.87	5	16.49	2	24.18	1	29.17	1	31.88
12	4	13.20	0.2	15.41	0.1	23.04	2	27.05	1	33.05
13	4	13.25	2	17.46	1	25.22	0	28.37	1	30.82
14	0.3	14.53	0	16.96	0	24.51	2	28.07	0	32.13

[a] Iintermolecular distance d is given in angstroms.

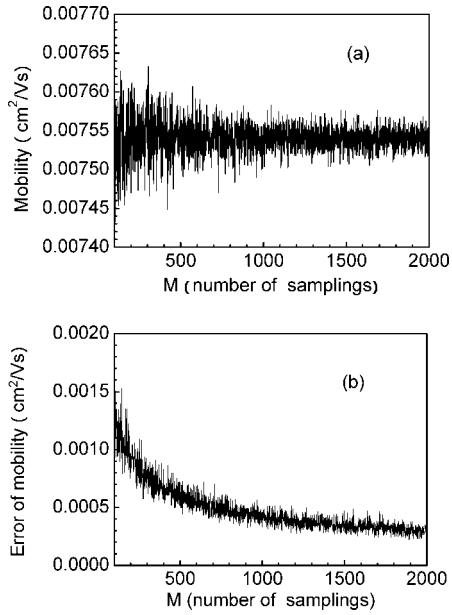

Figure 5. Simulated mobility (a) and its statistics error (b) vs the number of samplings for 6T/LT.

instance, the first four dimer pairs for 2T, 4T/HT, and 6T/HT have similar coupling values and intermolecular distances. They have the same relative orientations and solid-state packing structure. From Table 3, we find that the coupling values of 4T/LT, 6T/LT, and 8T are more regular than that of 3T and 7T. This is due to the molecular symmetry: the nT molecules for even n values have a C_{2h} point group, and their symmetry is higher than the 3T and 7T molecules (C_{2v} point group).

Room temperature mobility is obtained through a random walk simulation based on the Marcus rates. Typically, we made 2000 trajactories for the statistics treatment, and we compared these with the results from simulations of 40 000 trajectories. They agree very well (see Supporting Information). We give in Figure 5 the simulated mobility and the statistics error versus the simulation samplings for the case of the 6T/LT organic crystal.

We gather in Table 4 all the simulated mobilities and make a comparison with the available experimental results. It

Table 4. Theoretical Hole Diffusion Mobilities μ ($cm^2\ V^{-1}\ s^{-1}$) at Room Temperature ($T = 300$ K) for Oligothiophene Crystals[a]

molecular crystal	μ (theory)	μ (expt)
2T	0.0089 ± 0.00040	n.a.
3T	0.0040 ± 0.00020	n.a.
4T/HT	0.021 ± 0.0011	0.0025[b], 0.011–0.014[c]
4T/LT	0.0062 ± 0.00027	10^{-4}–0.006[d]
6T/HT	0.026 ± 0.0013	0.025[e], 0.03[f]
6T/LT	0.0075 ± 0.00028	0.002–0.009[e]
7T	0.0081 ± 0.00042	0.03[g]
8T	0.010 ± 0.00038	0.01–0.03[d]

[a] Available experimental data (LT or HT information not available) are listed for comparison. [b] Hajlaoui, R. et al.[14e] [c] Facchetti, A. et al.[39] [d] Katz, H. E. et al.[14d] [e] Servet, B. et al.[40] [f] Dodabalapur, A. et al.[41] [g] Nagamatsu, S. et al.[2b]

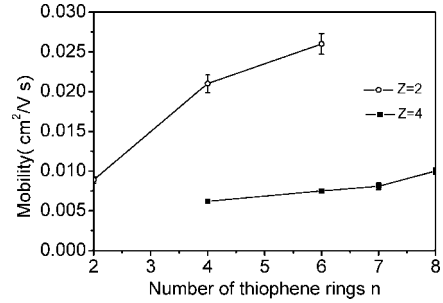

Figure 6. Drift mobility vs the number of thiophene rings (n).

should be noted that usually, the experimental measured mobilities can be very different from each other, as shown in Table 4. We find that the calculated values are reasonably close to all the measured values except for 7T. We note that 7T has not been widely studied. Thus, in Table 4, there is only one experimental value, instead of a range of values. Given such uncertainty in experiment, the theoretical estimate can provide some references.

We depict in Figure 6 the calculated room temperature hole mobility as a function of molecular size. The $Z = 2$ crystal structure leads to a larger drift mobility than that of $Z = 4$. For 6T, its two forms can be obtained by deposition in vapor growth: the HT form was observed above ~290° and the LT form below 280°.[42] The different phase could influence the mobility of the 6T films significantly:[40] a mobility as high as 0.025 $cm^2\ V^{-1}\ s^{-1}$ was achieved at a substrate temperature of 280 °C (near the melting point). When the substrate temperature (77 K, room temperature, 200 °C) decreases, the hole mobility in the range of 0.002–0.009 $cm^2\ V^{-1}\ s^{-1}$ is measured. The band structure calculations also show that the $Z = 2$ crystal leads to a larger bandwidth than the $Z = 4$ form. The largest dispersions in the HOMO bandwidth are 0.17 eV (α-4T/LT) and 0.45 eV (α-4T/HT), respectively.[38] This latter dispersion is similar to that found in α-6T/HT (0.42 eV).[35] The dispersion values are consistent with the transfer integrals presented in Tables 2 and 3.

We illustrate explicitly the packing structure for the dimer along the principal pathway, as well as the HOMO coefficients for the HT and LT phases of 4T and 6T in Figure 7. Note that the transfer integral is increased if both are bonding

(42) Kloc, C.; Simpkins, P. G.; Siegrist, T.; Laudise, R. A. *J. Cryst. Growth* **1997**, *182*, 416.

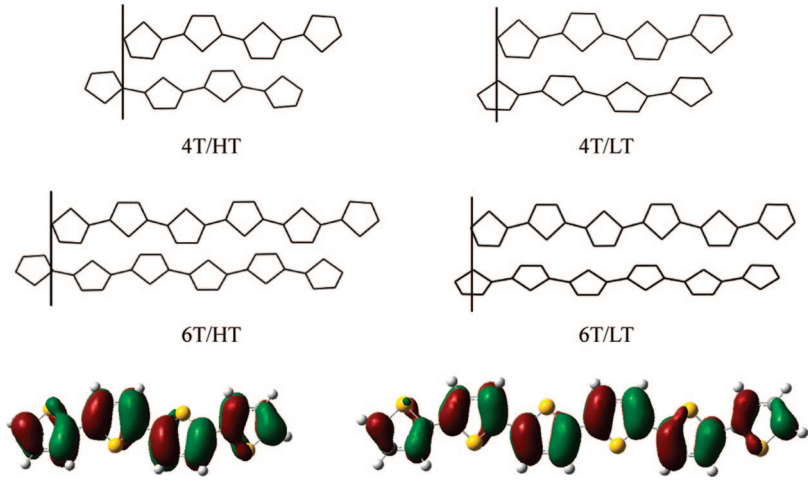

Figure 7. Intermolecular displacement taken from crystal packing along the long axis of thiophene for the dominant pathway. HOMOs of 4T and 6T also are shown.

or antibonding interactions between the π-atomic orbitals and decreased when there occurs a cancellation between bonding and antibonding overlaps. It is noted that for the LT phase, there exists a displacement of about half a thiophene ring width, while for the HT phase, the displacement is about one thiophene ring. Combined with the HOMO orbital charge distributions, one immediately rationalizes the fact that even though the intermolecular distances are almost the same, their transfer integral can differ about 2–3 times (compare Tables 2 and 3).

For all the $Z = 2$ crystals of oligothiophene, the electronic coupling terms are the largest, in the range of 34.48−39.95 meV. The obtained mobilities differ by a factor of 3: the reorganization energy is dependent on the conjugation length of the molecules. It decreases as the chain length increases (see Table 1).

Within the present simple model, the temperature-induced variation on V was neglected. As simulated through classical molecular dynamics recently by Troisi,[43] the thermal fluctuation disorder in organic solids is very large, which tends to reduce the mobility upon increasing the temperature. We note that thermal fluctuation in one dimension is particularly large. However, for a 3-D closely packed solid, such effects should be much less important. This deserves further study.

Finally, even though the crystal structure is employed here in defining all the charge diffusion pathways, the results also can be relevant for the thin films. In fact, in this approach, the charge is assumed to be localized in one molecule, instead of spreading out in the bulk. A good thin film is usually quite ordered up to a few hundred nanometers in size. The effects of grain boundaries and charge traps were neglected. For a pure crystal, if the intermolecular interaction is strong, the charge could not be assumed to be localized in the molecule; thus, the present model could not be applied. However, for the oligothiophenes we studied, we note that $V \ll \lambda$. Namely, the intermolecular coupling is much less important than the charge relaxation. Thus, Marcus theory is fully applicable, and the results presented in this work can shed light on materials design for organic semiconductors.

Conclusion

In this work, by assuming localized charge hopping described by the Marcus electron transfer model and a diffusion process simulated by the random walk technique, we theoretically investigated the influences of crystal packing and molecular size on the hole mobility of oligothiophenes 2T to 8T. Both the reorganization energy and the transfer integral were calculated at the first-principles DFT level. It was found that the longer conjugation chain favors the transport due to the smaller activation energy. Also, the high temperature crystal packing phase, or the $Z = 2$ crystal in general, favors the intermolecular electron coupling through favorable frontier orbital overlap.

Acknowledgment. This work was supported by the Ministry of Science and Technology of China (Grants 2006CB806200 and 2006CB0N0100), the NSFC, as well as the Chinese Academy of Sciences.

Supporting Information Available: Detailed descriptions concerning the random walk simulations from Marcus electron transfer rates to charge mobility, and procedures to estimate the simulation errors (PDF). This material is available free of charge via the Internet at http://pubs.acs.org.

CM8002172

(43) Troisi, A. *Adv. Mater.* **2007**, *19*, 2000.